

Extended Hubbard model: A cluster effective-medium approach

R. E. Lagos,* G. A. Lara,† and G. G. Cabrera

*Instituto de Física Gleb Wataghin, Universidade Estadual de Campinas (UNICAMP),
Caixa Postal 6165, Campinas 13081-970, São Paulo, Brazil*

(Received 6 April 1992; revised manuscript received 26 October 1992)

We present a cluster effective-medium approach to the extended Hubbard model, for the zero-temperature, half-filled-band paramagnetic phase. We recover the known limits and comment on the broadening corrections to the model, and find a first-order metal-insulator transition, resulting from both the cluster nature of the method and the correlated hopping term.

I. INTRODUCTION

The recent discovery of high-temperature superconductors¹ has, among other things, revived the interest in the Hubbard model² and the related Mott transition,^{3,4} a metal-insulator transition driven by electronic correlations. Such correlations are believed to be relevant to the onset of superconductivity in the high-temperature superconductors.^{1,5,6}

The standard model for correlated fermions exhibiting a metal-insulator transition was introduced by Hubbard,⁷ by means of a decoupling process of the Green's-functions hierarchy. Since Hubbard's papers, many techniques and approaches have been used to treat the Hubbard model and the metal-insulator transition; namely, variational,⁸ functional integral,⁹ Schwinger formalism,¹⁰ diagrammatic,¹¹ renormalization group,¹² Monte Carlo,¹³ alloy-analogy or coherent potential approximation (CPA),¹⁴ cluster,^{15,16} generalized CPA,¹⁷ and perturbation methods.¹⁸ Nevertheless, in spite of the vast amount of theoretical work cited above, the physical picture remains far from clear, due to the diverse, sometimes conflicting theoretical predictions, depending on the model and/or method used. In particular we mention non-Fermi-liquid behavior and the order (first- or second-order type) of the metal-insulator transition (for a review see Refs. 19 and 20).

In this paper we lay down the groundwork for a cluster effective-medium approach [a cluster CPA (Ref. 21)] to the extended Hubbard model for a single-band, nearest-neighbor (NN) tight-binding case, bringing into play the intersite (both diagonal and off-diagonal) Coulomb interaction terms. Our cluster CPA is indeed a cluster generalization of the alloy-analogy method,²² has the required analytic behavior,^{21,23} and reproduces the known results, namely, the band Hartree-Fock limit, the atomic limit, various diverse Hubbard's solutions,⁷ and probes inconsistencies in some of Hubbard's solutions.²⁴ Furthermore, we probe the consequences of performing quenched averages, an alloy-analogy feature, known to introduce uncontrolled approximations.²²

We consider the zero-temperature, half-filled-band paramagnetic phase, and find a first-order metal-insulator transition, supporting Mott's conjecture. This transition arises in our model as a consequence of both the cluster

nature of our cluster CPA and the inclusion of the correlated hopping Coulomb term.

II. EFFECTIVE-MEDIUM MODEL

We write the extended Hubbard model Hamiltonian^{5,15} as

$$H = H_S + H_D \quad (1)$$

with

$$H_S = \sum n_{i\sigma} \left[\varepsilon_0 + \frac{U}{2} n_{i-\sigma} + \frac{V}{2} n_{j-\sigma} \right],$$

$$H_D = \sum c_{i\sigma}^\dagger c_{j\sigma} [t - K(n_{i-\sigma} + n_{j-\sigma})],$$

where the c 's are the usual electronic destruction operators at site i (and NN j) with spin σ ; $n_{i\sigma}$ the number operator; ε_0 the site energy; U the intrasite and V the intersite (NN) Coulomb repulsion term, respectively; t the NN hopping integral; and K the off-diagonal Coulomb term. Notice, we have incorporated the parallel spin contribution of V via a Hartree-Fock scheme to the site energy term, so (1) becomes amenable to an alloy-analogy approach.^{7,22} If z denotes the number of NN, the half-bandwidth is $B = zt$, and with B as our energy unit, we define the following dimensionless parameters:

$$u = U/2B, \quad v = zV/2B,$$

$$\mathcal{H} = zK/B, \quad b = 1 - \mathcal{H}.$$

The standard Hubbard model corresponds to the particular case $v = \mathcal{H} = 0$; define the diagonal extended Hubbard model as the case $\mathcal{H} = 0$ and the full extended Hubbard model with all three u, v, \mathcal{H} finite. We write now the related Hamiltonian H_σ (of an electron gas with spin σ in a field of $-\sigma$ electrons),

$$H_\sigma = \sum W_i^\sigma n_{i\sigma} + \frac{1}{z} \sum W_{ij}^\sigma c_{i\sigma}^\dagger c_{j\sigma}, \quad (2)$$

where the summation is over sites (and NN sites) only, and with

$$W_i^\sigma = \varepsilon_0 + \frac{2u}{z} n_{i-\sigma} + 2v \sum n_{j-\sigma},$$

$$W_{ij}^\sigma = 1 - \mathcal{H}(n_{i-\sigma} + n_{j-\sigma})$$

the on-site and NN-site $-\sigma$ electron fields, respectively.

As in the alloy-analogy method, now generalized to a dimer,²¹ we replace H_σ by an effective H_σ^{eff} where the on (NN) -site fields are replaced by self-energy functions $\Sigma_{d(n)}(\omega)$. For the noninteracting case ($u=v=\mathcal{H}=0$) either Hamiltonian (1) or (2) reduces to a tight-binding Hamiltonian with on (NN) -site retarded Green's functions $G_{d(n)}(\omega, \varepsilon_0, B)$, where the G 's have explicit expressions according to the model used for the density of states (DOS).²³ Now for the effective Hamiltonian the on (NN) -site Green's functions are $G_{d(n)}(\omega, \Sigma_d, \Sigma_n)$. For the paramagnetic phase we do not need a spin index for the G 's and the Σ 's, and restrict hereafter our computation to Hubbard's DOS.

Now we define for the dimer both the Green's function and self-energy, both 2×2 matrices:

$$G = G_d + \sigma_x G_n,$$

$$\Sigma = \Sigma_d + \sigma_x \Sigma_n,$$

with σ_x the x Pauli matrix. The $-\sigma$ spin electron fields for the dimer (embedded in a virtual-crystal approximation environment^{21,22}) are given by the matrix W , with elements

$$W_{11} = \varepsilon_0 + 2(un_1 + vn_2),$$

$$W_{22} = \varepsilon_0 + 2(un_2 + vn_1),$$

$$W_{12} = W_{21} = 1 - \mathcal{H}(n_1 + n_2).$$

There are four static configurations, with $n_{1,2}=0$ or 1, and the cluster CPA condition²¹ requires

$$G(\omega, \Sigma) = \langle\langle [G^{-1}(\omega, \Sigma) + \Sigma - W(n_1, n_2)]^{-1} \rangle\rangle, \quad (3)$$

where $\langle\langle \rangle\rangle$ denotes configurational average.

From (3) we obtain the self-consistent equations for the self-energies $\Sigma_{d,n}(\omega)$, and (1) can be approximated²⁵ as

$$H \simeq H_\uparrow^{\text{eff}} + H_\downarrow^{\text{eff}} - E_c, \quad (4)$$

where E_c (a number) accounts for the potential energy being counted twice in this procedure. Notice that within the virtual-crystal approximation [i.e., inserting in (4) for the effective Hamiltonians expression (2), but with the W 's replaced by their configurational average], we recover the Hartree-Fock approximation for (1), and that the self-energy function is both energy and momentum dependent, i.e., nonlocal,^{18,26} given by

$$\Sigma(k, \omega) = \Sigma_d(\omega) + [\Sigma_n(\omega) - 1] \varepsilon_k^0 \quad (5)$$

with ε_k^0 the dispersion relation for the noninteracting system (centered at zero). For the half-filled-band case the solution of (3) has a symmetry best exhibited by taking $\varepsilon_0 = -u - v$. Incidentally, this energy shift is equivalent to defining the Fermi level $\varepsilon_F = 0$ and to setting the Hartree-Fock solution of (4) to the null solution $\Sigma_d(\omega) = \delta(\omega) = 0$ where $\delta(\omega) = \Sigma_n(\omega) - b$ is the band enhancement factor.

Let us define the following auxiliary matrices:

$$\sigma(\omega) = \Sigma_d + \delta(\omega)\sigma_x,$$

$$Q(\omega) = G^{-1}(\omega) + \sigma(\omega).$$

Furthermore, for any matrix of the type

$$\mathcal{M} = M_d + M_n \sigma_x \quad (M_{d,n} \text{ scalars}),$$

such as $G(\omega)$, $\Sigma(\omega)$, $Q(\omega)$, and $\sigma(\omega)$, we define the related scalar functions

$$M_\pm = M_d \pm M_n,$$

$$M_0^2 = M_d^2 - M_n^2 = \det(\mathcal{M}),$$

and the compact parameters

$$m_\pm = u + v \mp \mathcal{H},$$

$$m_0 = u - v.$$

From Eq. (3) we obtain the self-consistent equations satisfied by the self-energies

$$\sigma_\pm(\omega) = \frac{m_0^2 [Q_\pm^2 - m_\pm^2] + m_\pm^2 [Q_0^2 - m_0^2]}{Q_\mp [Q_\pm^2 - m_\pm^2] + Q_\pm [Q_0^2 - m_0^2]}, \quad (6)$$

where the ω dependence of the Q 's is implicit.

III. METAL-INSULATOR TRANSITIONS

Let us begin by writing down in a compact fashion the solutions Hubbard found to his model, namely, the HCPA solution (Hubbard's self-consistent solution incorporating scattering corrections to the Hubbard-I solution) and the HIII solution (Hubbard III solution, self-consistent solution incorporating both scattering and resonance broadening corrections).⁷ For that purpose we define

$$G_0(\omega) = G_d(\omega, \Sigma_d(\omega), b),$$

the Green's function at zero band enhancement.

Using the convention $\lambda=0$ for HCPA's and $\lambda=1$ for HIII's, Hubbard's solutions read

$$\Sigma_d(\omega) = u^2 [G_0^{-1}(\omega) + \Sigma_d(\omega) - \frac{1}{2}\lambda G_0(\omega)]^{-1}, \quad (7)$$

$$\delta(\omega) = 0.$$

We solve (7) using Hubbard's DOS and find at ε_F , with $\phi = \Sigma_n(0)/\Sigma_d(0)$,

$$\phi^2 = 4 \left[\left[\frac{u}{u_c} \right]^2 - 1 \right], \quad u \simeq u_c, \quad (8)$$

and with $u_c = \frac{1}{2}(\sqrt{3}/2)$ for the HCPA (HIII) solution.

The static configurational average in (3) regards the $-\sigma$ spin electrons as having infinite lifetime, at any given dimer configuration with dimer energy $W(n_1, n_2)$. The configurational average is a discrete sum, or an integral containing δ functions. In order to restore some dynamics (in a semiphenomenological fashion) we broaden the δ functions by replacing them by the distribution

$$f(\omega) = \begin{cases} 1/\Delta & \text{for } -\Delta/2 \leq \omega \leq \Delta/2 \\ 0 & \text{otherwise} \end{cases}$$

Solving for the CPA case, at ε_F and near the limit $\phi \simeq 0$ we find the same expression as in Eq. (8) but with $u_c^{-2} = 4(1-\Delta)$. The zero broadening case $\Delta=0$ reproduces the HCPA solution and the finite broadening $\Delta=2/3$ reproduces the HIII solution, at least near the limit $\phi \simeq 0$; thus HIII may be regarded as a (non-self-consistent) device to restore some dynamics to the CPA.

Referring back to Eq. (3), in the band limit ($B = \infty$ or $u = v = \mathcal{H} = 0$), we obtain $\Sigma(\omega) = \delta(\omega) = 0$, the same limit as obtained in the HCPA and HIII, namely the Hartree-Fock solution. The cluster CPA solution for the Hubbard model from (3) can be cast as

$$\begin{aligned} \Sigma_d &= (u^2 - \delta^2)(G_d^{-1} + \Sigma_d + \frac{1}{2}\delta\Sigma_n G_d)^{-1}, \\ \delta &= -u^4 Q_n^3 (Q_d^3 (Q_0 - u^2)^2 - Q_n^2 Q_0^2)^{-1}. \end{aligned} \quad (9)$$

For the limit of small bandwidth, near the atomic limit we expand the Green's functions in (9) and obtain the consistent result:

$$\delta(\omega) \simeq \Sigma_n(\omega) \simeq B$$

with

$$\Sigma_n(\pm\infty) = 1 \leq \Sigma_n(\omega) \leq \Sigma_n(0) = \frac{4}{3},$$

or equivalently

$$0 \leq \delta(\omega) \leq \frac{1}{3},$$

i.e., in the atomic limit the band enhancement $\delta(\omega)$ vanishes. Thus, at both the atomic and band limit, for the Hubbard model our cluster CPA solution retrieves the HCPA solution. For B small but not zero, we expand (9) to first order in $\delta(\omega)$, and obtain for Σ_d , an identical equation as in (7), except λ is replaced by $\delta(\omega)$.

Thus, HCPA underestimates band enhancements effects (but consistent within the CPA) and HIII overestimates band enhancements effects [by fixing $\delta(\omega) = 1$, a nonconsistent approximation in both CPA and cluster CPA schemes], introducing the HIII lack of consistency discussed in Ref. 24. We expand (7) for small ϕ , as defined right above Eq. (8) and obtain $\Sigma_n(0) = 4/3$, and an expression for ϕ similar to (8), but with a prefactor of 2.824 instead of 4 and with $u_c = 0.577$. If we were to mimic the cluster CPA with a CPA plus broadening as discussed above, we must assign to it a broadening factor $\Delta = 0.25$. We are tempted then to state, in light of the previous discussion, that as far as the values of u_c and Δ are concerned, HCPA (HIII) underestimates (overestimates) them, and cluster CPA's yield intermediate values, as shown in Table I.

Now the Hubbard model exhibits a metal-insulator transition of the band crossing type, an insulating phase materializes when a gap is open in the DOS at the Fermi level, thus the order parameter is the carrier density per site at ε_F and given by

$$n_F = -\frac{1}{\pi} \text{Im} G_d(0, \Sigma_d(0), \Sigma_n(0)).$$

For the standard Hubbard model it is found that the metal-insulator transition is a second-order transition, and near the transition $n_F \simeq \text{Im}\phi$. This behavior is con-

TABLE I. Solutions for the standard Hubbard model.

	u_c	Δ
HCPA	0.500	0.000
Cluster CPA	0.577	0.250
HIII	0.866	0.666

trary to Fermi liquid behavior, since the quasiparticle lifetime $\tau_{QP} \simeq -\text{Im}\phi^{-1}$ is finite at ε_F and indeed zero at the transition (in the metallic side, i.e., n_F nonzero). A first-order metal-insulator transition is predicted, following Mott's conjecture, with $\tau_{QP} = \infty$.³

For the diagonal extended Hubbard model our cluster CPA yields, from (3), $\Sigma_n(0) = 4/3$, and for small ϕ ,

$$\phi^2 \simeq \frac{(u^2 - v^2)^2}{u^2 + v^2} - \frac{1}{3}, \quad (10)$$

thus the Hubbard model in all the schemes (HCPA, HIII, and cluster CPA) and the diagonal extended Hubbard model in the cluster CPA, have the same type (apart from normalization factors) of metal-insulator transition discussed above (hereafter of the Hubbard type). Equations (8) and (10) are of the type $\phi^2 \simeq p^2 - p_C^2$, with p the transition driving parameter, a function of u and v . Then we have ϕ and an absolute value less than unity in the insulating phase ($p > p_C$) and ϕ pure imaginary in the metallic phase ($p < p_C$). In contrast, the behavior of a Fermi liquid, undergoing a Mott-type metal-insulator transition (hereafter of the Mott type), behaves as the Hubbard type in the insulating phase, but in the metallic phase ϕ is real, with an absolute value greater than unity.

In Fig. 1, we present a phase diagram (in $u-v$ space) for the diagonal extended Hubbard model, generalizing Bari's²⁷ result to the finite bandwidth case. The label Mott (Peierls) means the system is unstable to spin-(charge-) density waves, and the metallic phase is labeled

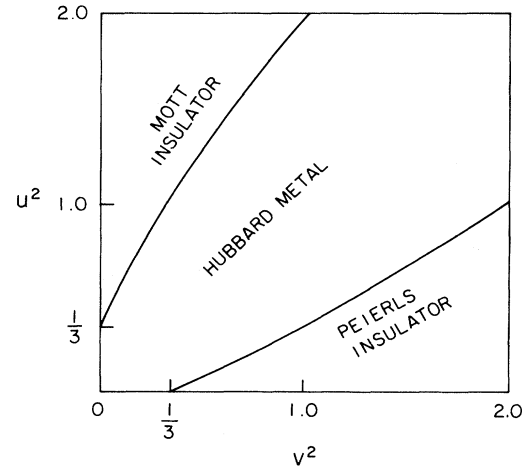


FIG. 1. Phase diagram ($u-v$ space) for the diagonal extended Hubbard model. Two insulating phases (one a Mott- and the other a Peierls-type insulator) at the corners, and a metallic phase of the Hubbard type (see text).

Hubbard, to distinguish it from a Fermi liquid metal. The Mott insulator region is given by

$$u^2 \geq v^2 + \sqrt{\frac{4}{3}(u^2 + v^2)},$$

and similarly the Peierls insulator region, interchanging u and v .

Finally, for the full extended Hubbard model, in light of our previous findings, we expand (3) for small ϕ and with $\theta = \Sigma_n(0) - 4b/3$, and obtain

$$\sum A_{nl}^i(u, v, \mathcal{H}) \phi^n \theta^l = 0 \quad (11)$$

with $i = 1, 2$ and $A_{00}^{1,2} = 0$.

The metal-insulator transition phase separation curve is

$$4A_{10}^1(u, v, \mathcal{H}) = \frac{b^2}{3}(m^2 + m_0^2) - 2m^2 m_0^2 = 0$$

with b, m_0 as previously defined and m given by

$$m^2 = (u + v)^2 + \mathcal{H}^2.$$

The insulating region is given by $A_{10}^1 < 0$ and, correspondingly, the metallic region by $A_{10}^1 > 0$. Near the transition we compute the remaining A 's, for $n \leq 4$ and $l \leq 1$. Near the transition all of them have definite signs and are different from zero; the terms labeled with the triad inl equal to 120, 140, 101, 121, 141, 211, and 231 are linear in \mathcal{H} for small \mathcal{H} . This last feature yields a qualitatively different transition as compared to the previously discussed cases. As the transition is approached, from the insulating side, both ϕ and θ vanish and $\text{Im}\phi = 0$, as in all previous cases, and from the metallic side two solutions are found by computing the solvability condition for the nonlinear algebraic system (11) in the variables ϕ, θ (see Ref. 28). For small but finite \mathcal{H} one solution vanishes at the interphase and the other remains finite. By continuity, we expect for small but finite \mathcal{H} to find a metal-insulator transition near the diagonal extended Hubbard model case, and by simple inspection of the vanishing solution near the latter, we discard it, since ϕ remains real, a feature not of a metal-insulator transition, a fortunate fact; otherwise, both solutions should be tested, selecting the physical one by minimizing the total energy, as given from (4). The finite solution corresponds to a first-order transition, confirming on more solid ground, both Caron and Pratt's findings (self-labeled as a zeroth-order approximation to the problem)¹⁵ and Mott's conjecture.³ Our metal-insulator transition for the full extended Hubbard model is neither of the Hubbard or Mott type.

In Fig. 2, we display ϕ^{-1} vs p (where the generic parameter p is a function of u, v , and \mathcal{H}). It is a first-order metal-insulator transition (as the Mott-type metal-insulator transition); nevertheless, the quasiparticle lifetime τ_{QP} is finite, but unlike the Hubbard-type metal-insulator transition it is not zero at the transition.

In Fig. 3, we plot the phase diagram for the full extended Hubbard model, parametrizing v as $v = \lambda u$. For any given λ the upper region corresponds to the insulating phase ($n_F = 0$) and conversely the lower region to the metallic phase (n_F finite for \mathcal{H} finite). Below the dashed line lays the parameter region for which $\tau_{\text{QP}} \geq \tau_H = 1$

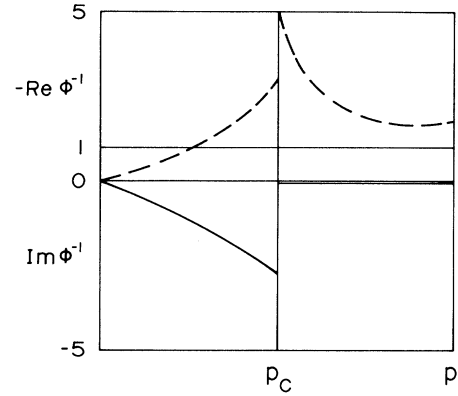


FIG. 2. The ratio $\phi^{-1} = \Sigma_d(0)/\Sigma_n(0)$ plotted vs a generic parameter p (a function of the Coulomb terms), exhibiting a metal-insulator transition (cluster CPA for the full extended Hubbard model; see text). $\text{Im}\phi^{-1}$ is displayed by the full line.

(hopping time), a region of physically meaningful, non-Fermi liquid type, quasiparticles.

In Fig. 4, with the same notation as in the preceding figure, we plot the jump of the DOS at the Fermi level n_F at the transition. The curves become steeper as \mathcal{H} increases, a feature that persists although in a tamed fashion if we solve the full equations (6) instead of the expansions (11). It is interesting to point out that no solutions are found for $\lambda < 0.012$ and $\lambda \geq 1$, a built-in safeguard, binding our parameters to the physical region $\mathcal{H} < 1$ and $\mathcal{H} < v < u$.

In Fig. 5, we sketch the hyperbolic tangent of the dc conductivity at zero temperature²⁶ for the several cases: (M) corresponds to Mott's conjecture, (C) to the full extended Hubbard model, and (H) to the Hubbard model (HCPA, HIII, cluster CPA) and diagonal extended Hubbard model. For the several solutions of the Hubbard model, we found the same qualitative behavior (a second-order transition); nevertheless, as broadening is introduced, the "residual differential conductivity"

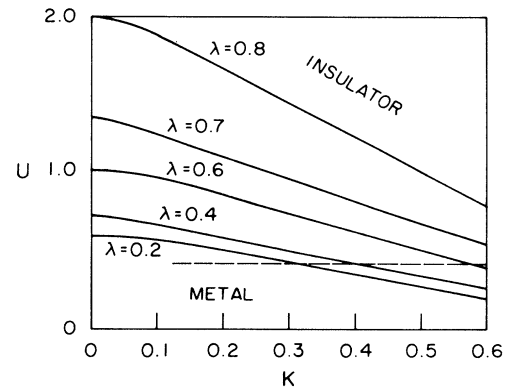


FIG. 3. Phase diagram for the full extended Hubbard model using the cluster CPA approach. Here $v = \lambda u$. For each λ value the upper (lower) region corresponds to the insulating (metallic) phase. The region below the dashed line indicates the parameter region where the quasiparticles have a lifetime greater than the hopping time (see text).

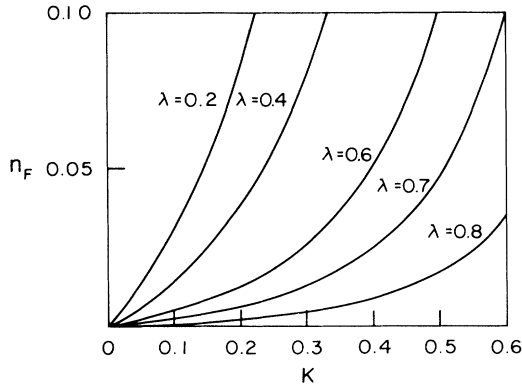


FIG. 4. The carrier density per site $n(\epsilon_F)$ discontinuity at the metal-insulator interphase, plotted vs \mathcal{K} and with $\lambda=v/u$ (see Fig. 3 and text).

(RDC) $\sigma_M - \sigma_H$ is reduced except at the transition point, where the RDC remains infinite. As for the C curve, which represents a first-order transition, as does M , the RDC $\sigma_M - \sigma_C$, although not infinite, is nonzero, a manifestation, we believe, of the approximation of dynamical averages by static (quenched) averages in the cluster CPA approach (a noncontrolled improvement over the CPA). A semiphenomenological restoration of the dynamics lost in the alloy-analogy procedure will reduce the RDC, may not change the character of the transition, but may also introduce some nonconsistent features, as discussed earlier for the HIII solution.

IV. CONCLUDING REMARKS

To conclude, let us summarize the present work. We developed a cluster CPA approach to the extended Hub-

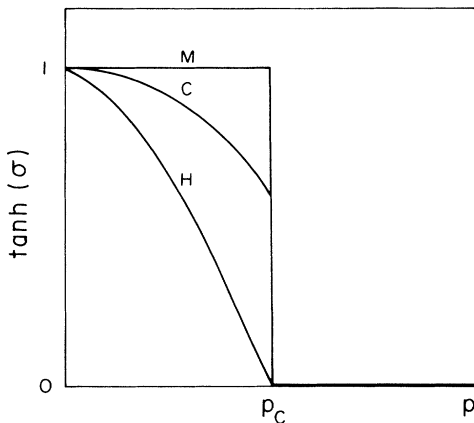


FIG. 5. The hyperbolic tangent of the dc conductivity $\tanh(\sigma)$ at zero temperature for the paramagnetic phase of the half-filled-band case. Mott's conjecture (M), the cluster CPA schematic result for the full extended Hubbard model (C); and the cluster CPA results for both diagonal extended and standard Hubbard models (H). The latter is a second-order metal-insulator transition, and the former two, first-order metal-insulator transitions (see text).

bard model, for the zero-temperature, half-filled-band paramagnetic phase, and found the following.

(i) Our cluster CPA is a self-consistent, analytic, straightforward method. We believe this method to yield a more controllable and systematic improvement of the single-site CPA, by allowing a dimer to be embedded in an effective medium, thus the NN Coulomb terms are treated in the same manner as the intrasite Coulomb term.

(ii) Configurational averages (in a virtual-crystal environment) remain quenched averages, but with the configuration space augmented twofold; noncontrolled approximations features such as the RDC issue, discussed at the end of the preceding section, persist,^{2,22} however, in a drastically reduced fashion, when compared for instance to the HCPA and HIII solutions, the RDC reduction being more substantial when we solve for the full extended Hubbard model.

(iii) It renormalizes the bandwidth and yields a nonlocal self-energy function $\Sigma(k, \omega)$, in contrast with the HCPA and HIII [band invariant, local $\Sigma(\omega)$]. We notice also that this local feature persists in generalized CPA's such as in Ref. 17, where the virtual-crystal environment is improved, yielding a first-order transition for the standard Hubbard model. We believe this to indicate that such an improvement procedure includes, somehow, correlated hopping effects.

(iv) Band renormalization effects vanish at the atomic and the band limit, thus recovering the HCPA and HIII results in those limits, and the Hartree-Fock results when applicable.

(v) Via our simple dynamics restoration procedure, we are able to compare some existing results, and display the limitations of the alloy-analogy method.

(vi) For the diagonal extended Hubbard model we found the spin-charge phase diagram, for finite bandwidth.

(vii) We found a first-order metal-insulator transition for the full extended Hubbard model, confirming previous preliminary calculations,¹⁵ Mott's conjecture,³ and abundant experimental data, when the driving mechanism is electronic correlations.³ The metal-insulator transition is first order, on account of the nonlocal $\Sigma(k, \omega)$ (a cluster effect) and the nonvanishing correlated hopping term \mathcal{K} , which incidentally is the only term to break the particle-hole symmetry for the half-filled-band case; otherwise, it is a second-order transition.

(viii) As a subsidiary result, we can map our results to a 50% simple binary alloy model. For a bipartite lattice, in a configuration of the type $(\alpha\beta)$, the latter means that any given site may be occupied by species α , with all NN's occupied by species β . Assume all configurations with equal probability and allow the species index to be either of the A or B type. We characterize the alloy model via a single-band tight-binding Hamiltonian; therefore, the relevant material parameters are the site energy $\epsilon(\alpha, \beta)$ and the NN hopping integral $t(\alpha, \beta)$. Then our results for the extended Hubbard model can be mapped to such an alloy model. The correspondence is achieved by setting $\epsilon(AB) - \epsilon(AA) = \epsilon(BA) - \epsilon(AB) = v$, $\epsilon(BB) - \epsilon(AA) = u$, $t(AB) = t(BA)$, and $t(AA)$

$-t(AB) = t(AB) - t(BB) = \mathcal{H}$. Furthermore, by mapping our results to this alloy model, we conclude that a transition from a single to a split band regime occurs as the parameters are varied, the transition occurring either in a continuous ($\mathcal{H}=0$) or discontinuous (nonvanishing \mathcal{H}) fashion.

We are extending the present work to probe the gap dependence on the Coulomb parameters. We consider finite temperature, band fillings other than half, and the cases of spin and charge ordered phases. Finally, the method presented here will be applied to Peierls-Hubbard and intermediate valence systems.

ACKNOWLEDGMENTS

This research work was partially supported by FAPESP (São Paulo), Project No. 91-2016-0. One of the authors (G.G.C.) is grateful to Conselho de Desenvolvimento Científico e Tecnológico (CNPq, Brazil) for partial financial support. Part of this work was completed while R.E.L. was visiting the Facultad de Ciencias, Universidad de Chile, Santiago de Chile, sponsored by Fondecyt, Project No. 91-0832. Also, R.E.L. acknowledges illuminating discussions with Professor Jaime Rössler.

*Present address: Departamento de Física, Instituto de Geociências e Ciências Exatas (IGCE), Universidade Estadual Paulista (UNESP), Caixa Postal 178, 13500-230 Rio Claro, São Paulo, Brazil.

[†]Present address: Departamento de Física, Pontifícia Universidade Católica de Rio de Janeiro, Caixa Postal 38047, 22452 Rio de Janeiro-RJ, Brazil.

¹*Theories of High Temperature Superconductivity*, edited by J. Woods Halley (Addison-Wesley, Reading, MA, 1988).

²T. V. Ramakrishnan, *Physica B* **163**, 34 (1990); D. M. Edwards and J. A. Hertz, *ibid.* **163**, 527 (1990); S. K. Sarker, H. R. Krishnamurthy, C. Jayaprakash, and W. Wenzel, *ibid.* **163**, 541 (1990); A. O. Anokhin, V. Yu Irkhin, and M. I. Katsnelson, *J. Phys. Condens. Matter* **3**, 1475 (1990).

³N. F. Mott, *Metal Insulator Transitions* (Taylor and Francis, London, 1974).

⁴D. Adler, in *Solid State Physics: Advances in Research and Applications*, edited by F. Seitz, D. Turnbull, and H. Ehrenreich (Academic, New York, 1968), Vol. 21, p. 116.

⁵G. A. Lara and G. G. Cabrera, *Solid State Commun.* **76**, 1121 (1990).

⁶R. E. Lagos, *Solid State Commun.* **79**, 323 (1991).

⁷J. Hubbard, *Proc. R. Soc. London, Ser. A* **276**, 238 (1963); **281**, 401 (1964).

⁸M. C. Gutzwiller, *Phys. Rev.* **137**, A1726 (1965); W. F. Brinkman and T. M. Rice, *Phys. Rev. B* **2**, 4302 (1970); M. I. Katsnelson and V. Yu Irkhin, *J. Phys. C* **17**, 4291 (1984).

⁹M. Cyrot, *Phys. Rev. Lett.* **25**, 871 (1970).

¹⁰T. Arai and M. H. Cohen, *Phys. Rev. B* **21**, 3300 (1980); **21**, 3309 (1980); T. Arai, *ibid.* **21**, 3320 (1980).

¹¹R. O. Zaitsev, *Zh. Eksp. Teor. Fiz.* **75**, 2362 (1978) [*Sov. Phys. JETP* **48**, 1193 (1978)].

¹²J. E. Hirsch, *Phys. Rev. B* **22**, 5259 (1980).

¹³S. Sorella, E. Tosatti, S. Baroni, R. Car, and M. Parrinello,

Int. J. Mod. Phys. B **2**, 993 (1988); S. Sorella, A. Parola, M. Parrinello, and E. Tosatti, *Europhys. Lett.* **12**, 721 (1990); F. F. Assad, *Helv. Phys. Acta* **63**, 580 (1990); L. Chen, C. Bourbonnais, T. Li, and A. M. S. Tremblay, *Phys. Rev. Lett.* **66**, 369 (1991).

¹⁴M. Cyrot, *J. Phys. (Paris)* **33**, 125 (1977); *Physica* **91B**, 141 (1977); E. N. Economou, C. T. White, and R. R. de Marco, *Phys. Rev. B* **18**, 3946 (1978).

¹⁵L. Caron and G. W. Pratt, Jr., *Rev. Mod. Phys.* **40**, 802 (1968).

¹⁶A. Montorsi and M. Rasetti, *Mod. Phys. Lett. B* **4**, 613 (1990).

¹⁷M. Corrias, *Mod. Phys. Lett.* **4**, 549 (1990); *Int. J. Mod. Phys. B* **5**, 1015 (1991).

¹⁸A. P. Kampf, *Phys. Rev. B* **44**, 2637 (1991); H. Schweitzer and G. Czycholl, *Z. Phys. B* **83**, 93 (1991).

¹⁹*The Hubbard Model*, edited by M. Rasetti [*Int. J. Mod. Phys. B* **5**, issues 6/7 (1991)].

²⁰C. Herring, in *Magnetism*, edited by G. T. Rado and H. Suhl (Academic, New York, 1966), Vol. 4; D. M. Edwards and A. C. Hewson, *Rev. Mod. Phys.* **40**, 810 (1968).

²¹R. E. Lagos and R. Friesner, *Phys. Rev. B* **29**, 3045 (1984); *J. Lumin.* **31/32**, 618 (1984); *Chem. Phys. Lett.* **122**, 98 (1985).

²²B. Velický, S. Kirkpatrick, and H. Ehrenreich, *Phys. Rev.* **175**, 747 (1968); G. Czycholl, *Phys. Rep.* **143**, 277 (1986).

²³R. E. Lagos and R. Friesner, *J. Phys. C* **20**, 4833 (1987).

²⁴J. Rössler, R. Ferrer, and B. Glass, *Phys. Status Solidi B* **93**, K33 (1979).

²⁵F. Brouers, *Phys. Status Solidi B* **76**, 145 (1976); A. K. Gupta, D. M. Edwards, and A. C. Hewson, *J. Phys. C* **8**, 3207 (1975).

²⁶G. Rickayzen, *Green's Functions and Condensed Matter* (Academic, New York, 1980).

²⁷R. A. Bari, *Phys. Rev. B* **3**, 2662 (1971).

²⁸J. V. Uspensky, *Theory of Equations* (McGraw-Hill, New York, 1948).